J. Fluid Mech. (1975), *vol.* 69, *part* 2, *pp.* 229–240
Printed in Great Britain

The starting flow down a step

By H. HONJI
Research Institute for Applied Mechanics, Kyushu University,
812 Fukuoka, Japan

(Received 16 September 1974)

The incompressible starting flow past a downstream-facing right-angled step was investigated at Reynolds numbers R (based on step height) less than 500 by means of flow-visualization techniques. The distance between the step and the point of reattachment on the downstream wall was found to increase linearly with time at intermediate stages of the flow development. The recirculation region formed behind the step was composed of three vortex domains at earlier stages of its development when $R \gtrsim 140$. It was observed for $R \gtrsim 200$ that once the starting vortices had been shed downstream a steady recirculation region was established. The evolution of filaments of tracer in the flow down the step was found to vary considerably with R. The filaments were observed to develop faster in the flow down the step than in that past a symmetric model without a downstream wall when $R \gtrsim 140$.

1. Introduction

Many papers have been concerned in a variety of ways with incompressible flow past a downstream-facing 90° step. The general features of the flow are separation of a shear layer at the corner, its reattachment to the surface of the downstream wall and the formation of a circulation region immediately behind the step.

Tani, Iuchi & Komoda (1961) and Roshko & Lau (1965) made pressure measurements in the reattachment region at high Reynolds numbers; Roshko & Lau proposed a criterion for laminar reattachment. Transition of a shear layer before reattachment was investigated by Goldstein *et al.* (1970) in more detail. Numerical experiments on two-dimensional flow down a step were made by Gerrard (1972). Starting from assumed initial conditions, he found the development of some characteristic quantities of the flow, and revealed the effect of disturbances on the oscillation of the recirculation bubble at a Reynolds number of 100.

This problem is closely related to the study of the flow past a bluff body with a splitter plate which interferes with the exchange of vorticity of opposite signs. The importance of the vorticity exchange in the formation of a periodic wake was examined in detail by Gerrard (1966) on the basis of the two characteristic lengths, the length of the formation region and the diffusion length of the free shear layer. Bearman (1965) investigated the effect of a splitter plate in the wake behind a bluff body on vortex shedding at a Reynolds number of about $2{\cdot}5 \times 10^5$,

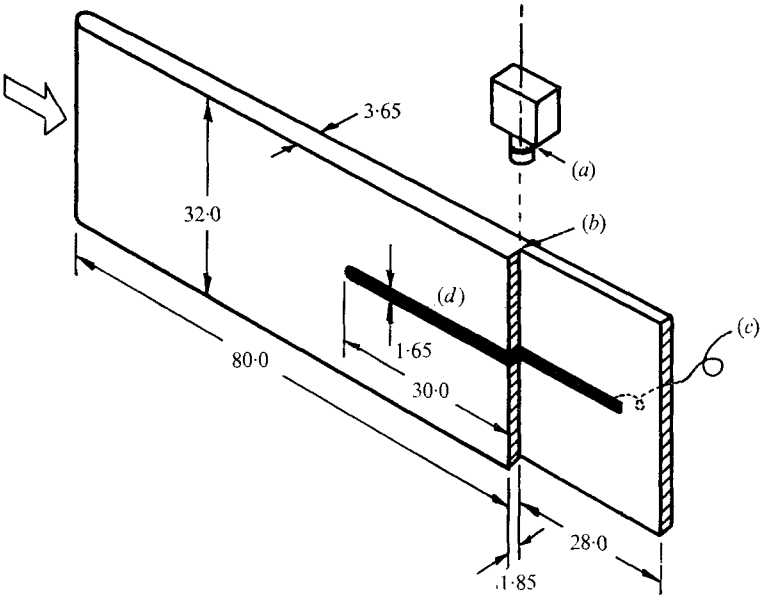

FIGURE 1. Experimental set-up (dimensions in cm). Arrow indicates the flow direction relative to the model. (*a*) Camera, (*b*) step, (*c*) d.c. power supply, (*d*) brass strip.

and found that there is no pronounced periodicity of vortex shedding if the plate length exceeds about three step heights. De Brederode & Bradshaw (1972) showed that nominally two-dimensional flow down a step has a strongly three-dimensional structure at high Reynolds numbers.

This work is concerned with the starting flow down a step at Reynolds numbers, based on step height, less than 500. It has been shown by Honji & Taneda (1969) and Taneda & Honji (1971) that the wakes of symmetric bodies performing unsteady motions have many characteristic features different from those proper to steady or mean turbulent wakes. No experiments, however, seem to have been made on the laminar starting flow down a step. The main purpose of the experiment is to reveal the fine-structure of the time-dependent recirculating flow behind the step, but some other features are also discussed in relation to the existing results mentioned above.

2. Experimental methods

The experiment was made using a water tank of width 75 cm, depth 35 cm, and length 400 cm. The tank was equipped with a motor-driven carriage which could be started impulsively at a constant speed between about 0·1 and about 10 cm/s by means of a dog-clutch coupling system. This coupling system made it possible to establish steady motion of the carriage in a very short time compared with that taken by the flow to develop.

The test body for providing a precisely right-angled downstream-facing step was made of polycarbonate plates. Its overall length in the flow direction was

108 cm while the step height was 1·85 cm, as shown in figure 1. The length of the upstream plate was 80·0 cm, which was chosen by taking account of the time required for the starting process to be completed. The test body was attached to the carriage vertically and towed in the water tank. The vertical span of the test body was 32 cm and its leading edge was rounded smoothly to avoid separation of the oncoming stream at the edge. The distance between the surface of the upstream plate and the facing side wall of the tank was 35·0 cm, being equal to 19 step heights approximately. It should be noted that the flow speed relative to the model is slightly larger than the towing speed U, because of the presence of the two side walls of the water tank. The wall effects, however, are not considered, and the Reynolds number R is here defined as Uh/ν, where U, h and ν are the speed of the model, the step height and the kinematic viscosity of water, respectively.

The electrochemical method was used for flow visualization: white smoke of metallic compounds was educed electrochemically from the surface of a thin brass strip which had solder smoothly applied on its surface. The brass strip was embedded in the surface of the upstream main plate on its centre-line. The strip was 1·65 wide, 0·3 cm thick and 30 cm long. Another, slightly shorter strip was embedded in the downstream main plate similarly. These brass strips were used as a couple of anodes. A cathode made of the same material was placed 30 cm downstream from the step. D.c. power of 50 V and 60 mA was supplied between the anodes and the cathode. The smoke which emanated from these strips made it possible to observe the filament development without disturbing the water before starting. The aluminium-dust method was also used in order to observe the streamline evolution.

The horizontal layer of water on the same level as the brass strip mentioned above was illuminated with a 1 kW slide projector, and after the beginning of motion the developing flow patterns were photographed consecutively with a camera fixed to the carriage on top of the step. The exposure time ranged from 0·4 to 8 s, and the mid-time of exposure is here referred to as the 'time of observation' t since the start of the motion.

The flows were fairly two-dimensional over the range of Reynolds numbers examined, except immediately behind both edges of the step, as can be seen in figure 2 (plate 1). As described above, all the photographs were taken with the camera fixed with respect to the test body, except figure 2, which was taken with the camera at rest with respect to the undisturbed water. Flow directions are from left to right in all the photographs given in this paper.

3. Experimental results

The starting flow down a step is characterized by the Reynolds number R and the dimensionless time Ut/h. This is valid only if the initial disturbance caused by the leading edge of the step model has not been reached by the step. After the whole distance between the leading edge and the step has been travelled by the step, the flow pattern depends not only on this distance but also on the front shape of the model: these determine the thickness of the boundary layer

before separation at the step. The boundary-layer thickness δ increases with time approximately as $\delta \approx 3{\cdot}66(\nu t)^{\frac{1}{2}}$, as long as t is not large if the flow speed at the boundary-layer edge is defined as $0{\cdot}99U$ and the upstream wall is regarded as infinite.

Immediately after the onset of motion, potential flow is established around the model, then a boundary layer begins to grow on the surface of the model as the vorticity diffuses. The developed shear layer separates at the upper corner of the step and reattaches to the surface of the downstream wall. The point of reattachment moves downstream with time as the recirculation region extends downstream.

The streamline development with time is shown in figures 3–5 (plates 1 and 2) for three different values of R. In some of these figures streaklines are superposed on the streamlines. When R is not large, a single separation bubble is formed behind the step as shown in figure 3. The starting process at a larger value of R is shown in figure 4. In figure 4 (*b*), the formation of a couple of secondary vortices can be seen behind the step. The secondary vortex behind the lower corner is formed as a result of shear-layer separation, which is induced by the reverse flow along the surface of the downstream wall. A similar secondary flow was observed by Bearman (1965) in a mean turbulent flow past a bluff body with a splitter plate. The secondary vortex behind the upper corner is formed as the separated shear flow begins to be deformed by the secondary vortex growing in the lower corner. The critical value of R for the appearance of the laminar secondary vortex in the lower corner is about 120, and that for the appearance of a couple of secondary vortices is about 140. The secondary vortices die away with time at low Reynolds numbers. The vortex centres can no longer be pin-pointed in the final state of the flow shown in figure 4 (*c*).

The starting process at a further large value of R is shown in figure 5, where (*a*), (*b*) and (*c*) show the formation of a small secondary vortex at an early stage, the division of the recirculation region into three distinct vortex domains and the eventual shedding of these starting vortices, respectively. The main vortex and the vortex immediately behind the upper corner have a clockwise direction of rotation while the remaining one in the lower corner has a counterclockwise direction of rotation. These vortex domains become more distinct as R is increased. The secondary vortices formed behind the step are very similar in nature to those which were found by Honji & Taneda (1969) in the starting flow past a circular cylinder at Reynolds numbers based on the cylinder diameter larger than about 500.

When R was larger than about 200, it was observed that the starting vortices could no longer remain stationary behind the step: the rear part of the main vortex was shed downstream. After this, however, a very large recirculation region was established behind the step, as will be seen from figure 6 (plate 3). The formation of a couple of secondary vortices may have some connexion with the shedding of the main starting vortex, although the critical values of R (140 and 200) for the appearance of both phenomena are different. This difference, however, should be attributed to the plausible idea that the shedding of the main vortex requires the secondary vortices to have a certain intensity. In fact, the

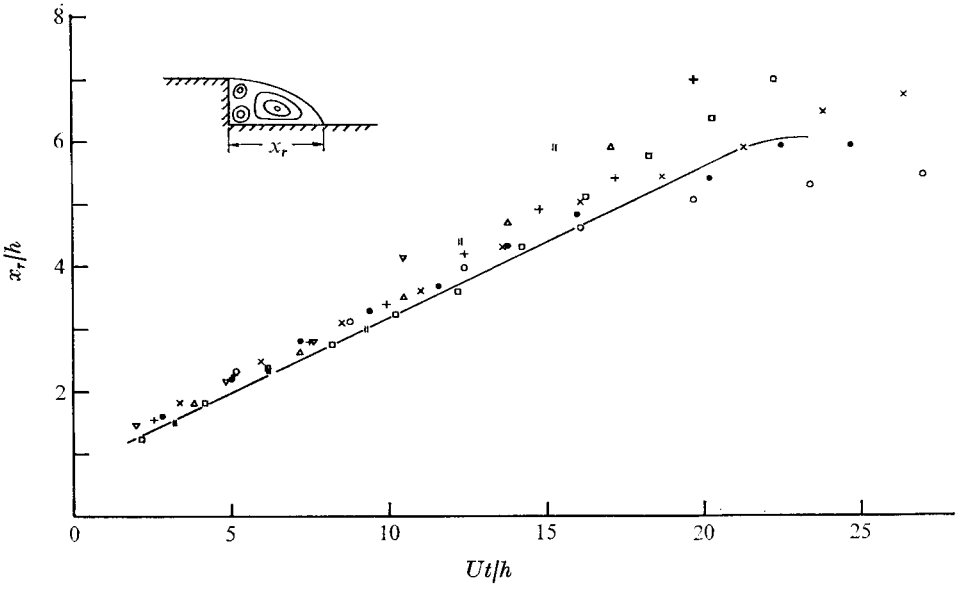

FIGURE 7. Movement of the reattachment point with time. ——, numerical prediction by Gerrard (1972).

	○	●	×	□	+	△	‖	▽
R	99·6	126	153	200	223	304	398	412

secondary vortices attached directly to the step seem to play a role in pushing the main vortex downstream before the establishment of a steady recirculation region, when R is large enough ($R \gtrsim 300$).

In figure 7, the dimensionless distance x_r/h between the step and the reattachment point is plotted against Ut/h. The value of x_r increases linearly with Ut, the distance travelled by the step, in the intermediate stages of the flow development. Immediately after the beginning of motion, the reattachment point takes a time less than $2h/U$ to move down from the upper to the lower corner of the step. The numerical result obtained by Gerrard (1972) at $R = 100$ is indicated by the solid line. The experimental data fit the numerical prediction approximately over the range of Ut/h presented in the figure; the neglect of wall effects seems to be responsible for the slight discrepancy. The starting process is completed during a dimensionless time interval of about 25. The distance travelled by the model during this interval is about 46 cm, which is much shorter than the overall length of the upstream wall in the flow direction.

The results given above were obtained mainly from examination of streamline patterns. Some remarks should be made here on flow visualization using dye elements in a time-dependent flow. As is well known, streamlines do not coincide with streaklines when the flow is not steady. The dye elements represent streaklines if they are introduced at one or more specific points in a flow field. In this experiment, the filament separating from the upper corner is considered to show the streakline evolution, when the diffusion of dye is not dominant. As will be seen from figures 12 and 14 (plates 4 and 5) below, the filaments were well

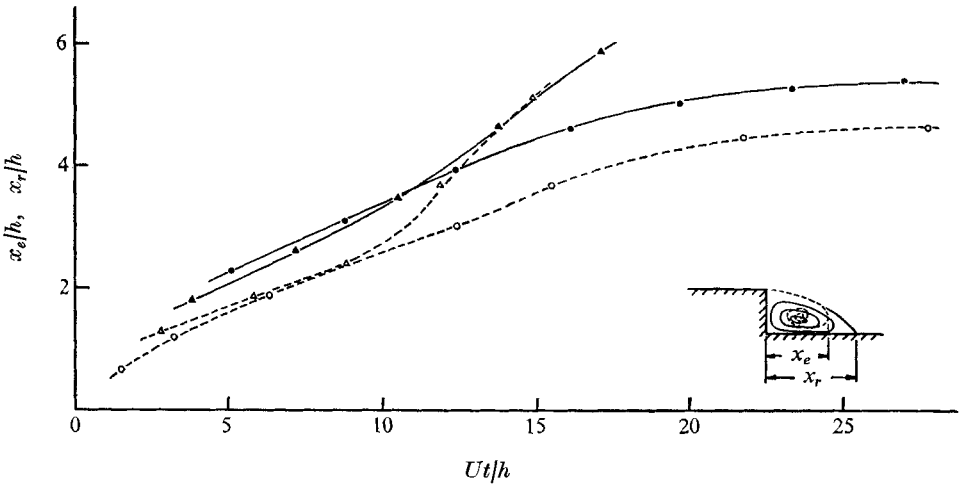

FIGURE 8. Comparison of the development of filaments and streamlines. △, ▲, $R = 303$; ○, ●, $R = 97$; ———, x_r/h, streamline; – – – –, x_e/h, streakline.

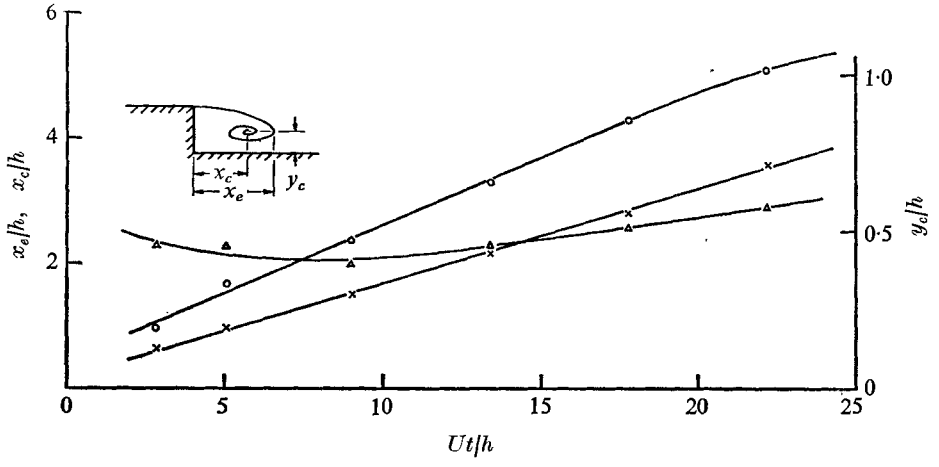

FIGURE 9. Timewise evolution of characteristic quantities for a filament at $R = 142$. ○, x_e/h; ×, x_c/h; △, y_c/h.

preserved until the later stages of their development. A filament also separates from the surface of the downstream wall when R is larger than about 120, the critical value for the formation of a laminar secondary vortex. This line does not show a streakline in its true sense because the separation point moves along the surface of the wall with time. However, this filament can also be approximately regarded as a true streakline at intermediate stages of its development, because the movement of its separation point is very slow, as will be seen from figures 12 (*b*)–(*d*).

Figure 8 shows a comparison of the development of both streamlines and streaklines at two different Reynolds numbers: x_r and x_e are the distance between the step and the reattachment point of the dividing streamline and the distance between the step and the rear end of the streakline, respectively. The curve

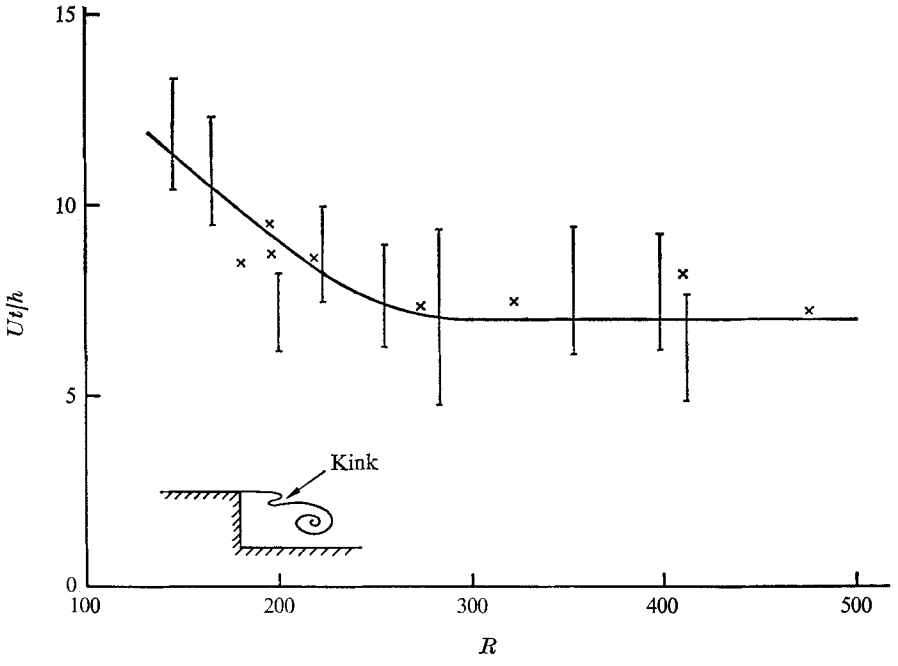

FIGURE 11. Reynolds number dependence of the value of Ut/h at which a kink in the filament first appears. ⊢—⊣, photographic observation; ×, visual observation.

for x_r/h is approximately parallel to the curve for x_e/h at $R = 97$. At $R = 303$, however, the end of the filament begins to move quickly downstream at about $Ut/h = 10$, because of the starting-vortex shedding at larger Reynolds number.

An example of the development of some characteristic quantities for the filament at $R = 142$ is given in figure 9. x_c and y_c indicate the instantaneous positions of the vortex centre as shown in the figure. At earlier stages of the vortex development, a kink in the filament always appears when R is not small. Figure 10 (plate 3) shows a comparison of filaments and streamlines at two different Reynolds numbers. The filament shown in figure 10(*b*) has a kink on the upstream side of the main vortex. The critical range of R, between 135 and 146, for the formation of the kink is approximately equal to the range of R in which the three vortex domains begin to be formed. This means that the kink in the filament is caused by the formation of secondary vortices behind the step. In figure 10(*b*), however, the secondary vortices have already merged into a main recirculation region, because the kink appears slightly later and the secondary flow is very weak in this critical range of R. The dimensionless time at which the kink first appears is plotted against R in figure 11. From this figure, it will be seen that the critical value of Ut/h decreases with R up to about $R = 300$, and settles down to about 7·0 for $R \gtrsim 300$.

The development of filaments at a relatively large Reynolds number is shown in figure 12. As R is increased, the kink in the upper filament leads to partition of the main vortex from the secondary vortex region behind the step, as may be seen from figure 12(*b*). The flow shown in figure 12(*b*) corresponds to

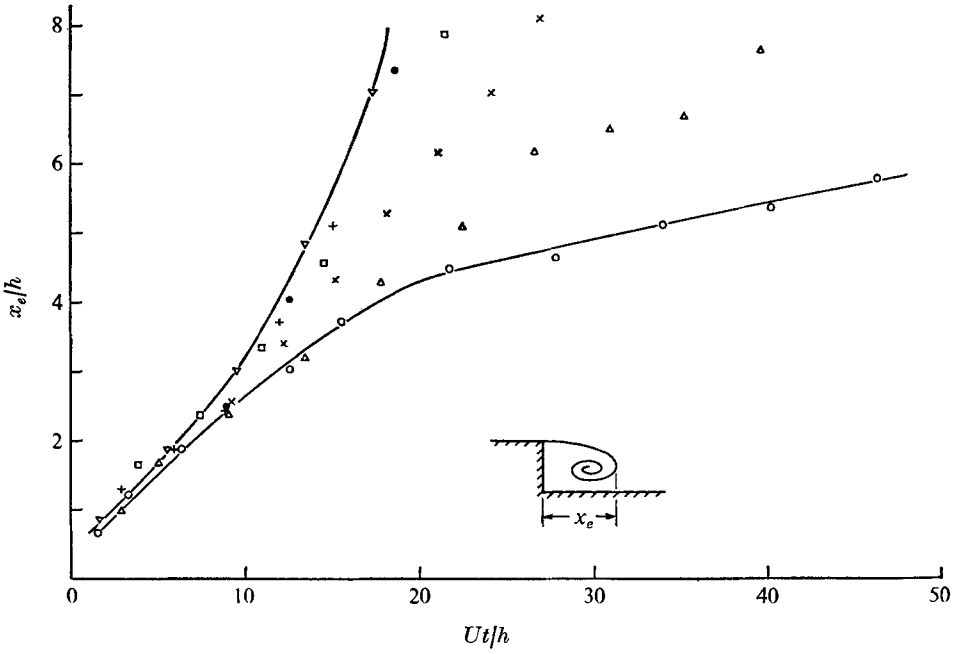

FIGURE 13. Reynolds number dependence of the filament development for the step model.

	○	△	×	□	+	●	▽
R	94·8	142	190	234	303	379	474

the streamline pattern shown in figure 5(*b*), where the formation of three distinct vortex domains is displayed. In figure 12(*c*), the starting main vortex is elongated and its downstream part is about to be shed. The filament emanating from the wall downstream develops very slowly, but eventually merges into a steady recirculation bubble. The development of a filament is shown quantitatively in figure 13, in which the motion of the rear end of the filament is seen to vary considerably with R. This is not improbable because many complicated processes occur when R increases, as mentioned above.

In the course of the experiment, vortex shedding was observed at larger values of Ut/h with R up to about 1000, but no vortex shedding with a characteristic frequency was observed on the downstream wall. The length of the downstream wall was about 15 step heights, which exceeded by far the critical length of 3 step heights given by Bearman (1965), although R is different.

If the mixing of two shear layers separated from either side of a bluff body is once allowed, the recirculation bubble begins to oscillate at a later stage of the development of the starting flow, and eventually vortices begin to be shed alternately. An experiment was carried out on the flow past a symmetric bluff body, which was made by cutting off the downstream wall of the step model precisely at the step. Figure 14 (plate 5) shows the development of a filament behind the symmetric model without a downstream wall. The Reynolds number R given here is based on $h = 1{\cdot}83$ cm, half the thickness of the model. Dye

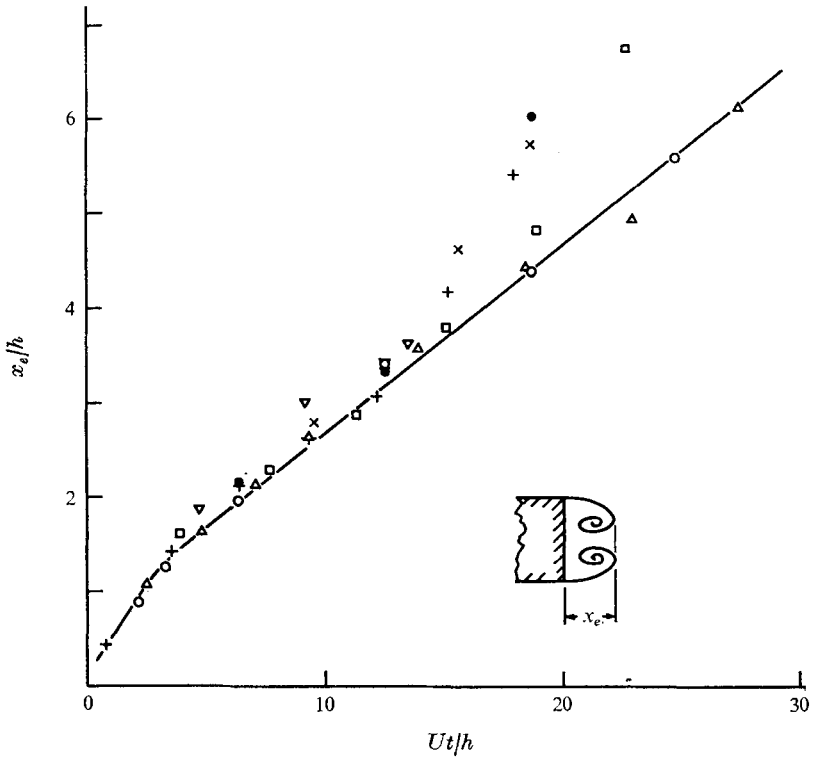

FIGURE 15. Reynolds number dependence of the filament development for the symmetric model. ——, $R = 142$.

	○	△	□	+	●	▽
R	94·8	142	234	302	378	472

elements were introduced only from an upper side of the model. The beginning of wake oscillation and the alternate shedding of vortices are clearly seen in figures 14(*d*) and (*e*), respectively. In figure 14(*d*) the dye elements are already spread over the whole region of the wake. Unlike the flow down a step, no evidence is seen of the formation of any secondary vortices. Figures 12 and 14 were taken at the same dimensionless times.

The movement of the rear end of a filament with time is shown in figure 15. Compared with the case of the step model, the experimental data collapse well on to a single curve when Ut/h is not large. This suggests that the filaments are convected smoothly downstream by the external flow. In figure 16, the development of filaments for these two different models are compared directly at $R = 94{\cdot}8$, 142 and 234. The filaments develop more quickly for the step model when $R > 142$, and for the symmetric model when $R < 142$. At $R = 142$ they develop approximately similarly. Perhaps this result is correlated with the appearance of secondary vortices at about the same Reynolds number. The secondary vortices are considered to promote the downstream stretching of filaments.

The critical time at which the laminar regime of starting flow begins to

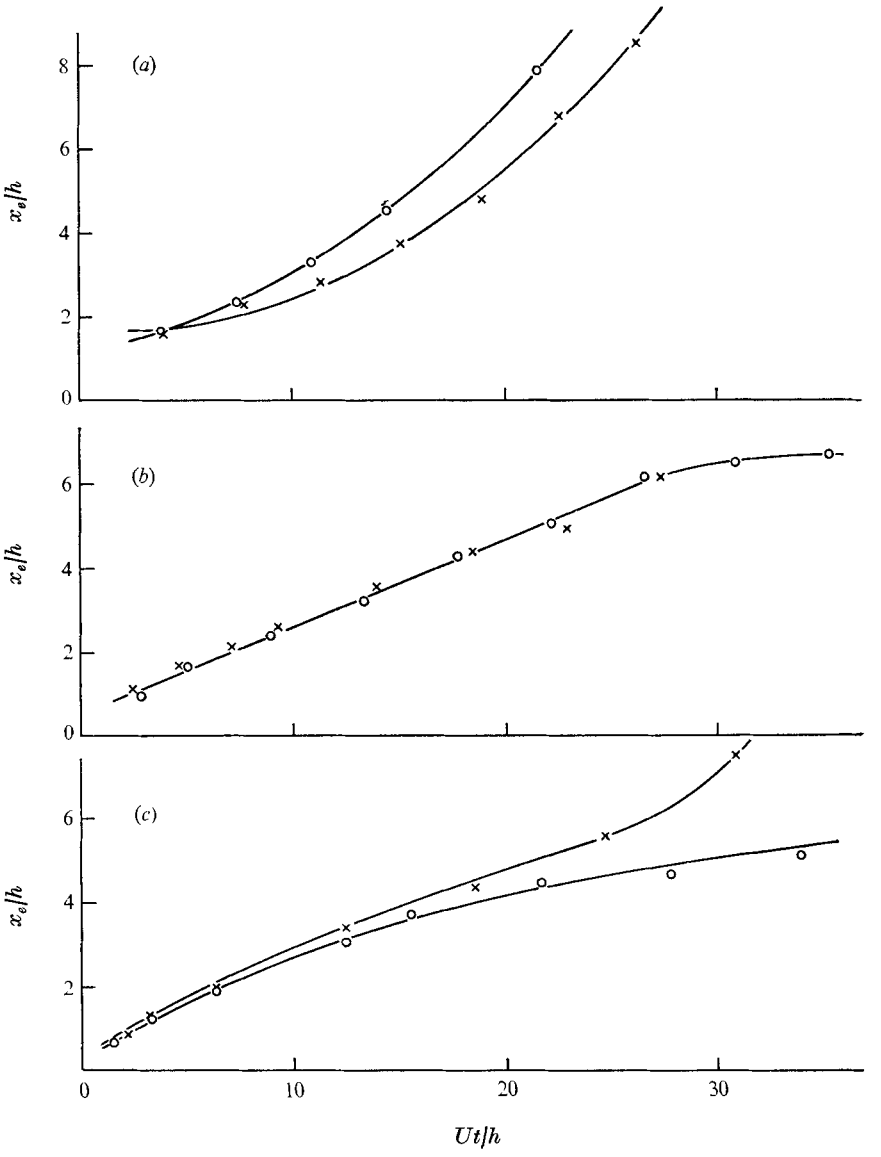

FIGURE 16. Comparison of the downstream movement of the rear ends of filaments for the two different models. (*a*) $R = 234$, (*b*) $R = 142$, (*c*) $R = 94{\cdot}8$. ○, step model; ×, symmetric model.

collapse is plotted against R in figure 17. For the flow at $R \gtrsim 200$, this is the time at which the vortex centre first becomes not clearly defined. This time is approximately equal to the time at which the shedding of the main vortex starts; for the flow past a symmetric model only this criterion is employed for the determination of the critical time, irrespective of the range of R. For the flow at $R < 200$, the time is taken as that at which the steady recirculation region is first established. The values of Ut/h lie between about 12 and about 30 over the range of R

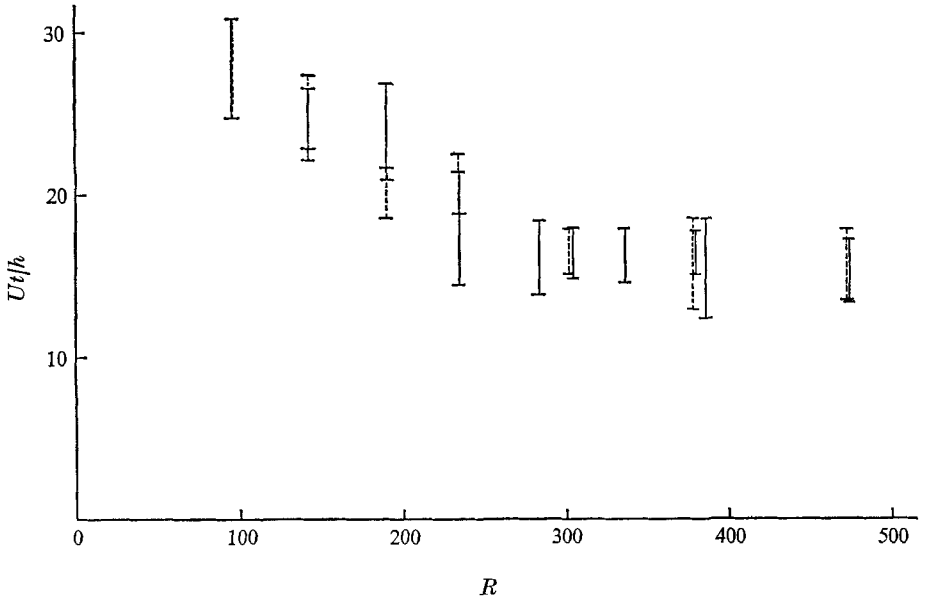

FIGURE 17. Reynolds number dependence of the value of Ut/h at which the laminar starting vortex begins to collapse ($R \gtrsim 200$) or steady-state flow is established ($R < 200$). ⊢——⊣, step model; ⊢– – –⊣, symmetric model.

examined. At $R > 300$, Ut/h becomes approximately constant at about 16. A remarkable feature is that the starting laminar flow begins to collapse almost at the same time for both the models, in spite of the different manner of vortex development shown in figure 16. The process of starting-vortex disintegration may not be dominated by the mixing of two shear layers, which always plays an essential role in the formation of an oscillating wake.

4. Conclusions

A visualization study was carried out of starting flow down a step at low Reynolds numbers. Specific comments and conclusions are as follows.

(i) After the onset of motion, a recirculation region begins to form behind the step. The point of reattachment moves downstream approximately linearly with time. The starting flow is fairly two-dimensional.

(ii) When R is larger than about 120, a secondary vortex appears in the lower corner of the step. The appearance of this localized vortex is due to separation of a shear layer caused by the main recirculating flow on the surface of the downstream wall.

(iii) When R exceeds about 140, the recirculation region is composed of three vortex domains at earlier stages of the flow development. Two of them are in clockwise rotation, and the remaining one is in counterclockwise rotation. The domains become more distinct as R is increased. The appearance of these vortices leads to the formation of a kink in the filament separating from the upper

corner. The critical time at which the kink first appears decreases with increases of R up to about 300, and becomes constant at about $Ut/h = 7{\cdot}0$ for $R > 300$.

(iv) The starting recirculation bubble develops into the steady recirculation region continuously when R is not larger than about 200. At larger Reynolds numbers, the steady recirculation is established after the starting vortices are shed downstream.

(v) The time-dependent filament evolution shows a rather simpler R dependence for the symmetric model without a downstream wall than for the step model. However, the wake formed behind the symmetric model begins to oscillate at a later stage of its development.

(vi) For the step and symmetric models, the filament develops with time similarly for an R of about 140. The development is faster for the symmetric model when $R < 140$, and for the step model when $R > 140$.

(vii) For both models, the critical value of Ut/h at which the laminar starting vortices begin to collapse is about 16 over the range $300 \leqslant R \leqslant 500$.

The investigation was carried out at the Department of the Mechanics of Fluids, University of Manchester, where the author was a visiting research fellow during 1973/1974. The author would like to express his sincere thanks to Dr J. H. Gerrard for his invaluable suggestions and discussions during the course of this work. The author also wishes to express his cordial gratitude to Professor N. H. Johannesen and the staff of the Department of the Mechanics of Fluids for their warm hospitality and continued interest in this work. The experiments were made with apparatus provided by a Science Research Council grant, which is gratefully acknowledged. The author is indebted to the Ministry of Education of Japan for the Research Fellowship.

REFERENCES

BEARMAN, P. W. 1965 *J. Fluid Mech.* **21**, 241.

BREDERODE, V. DE & BRADSHAW, P. 1972 *Imperial College Aero. Rep.* no. 72–19.

GERRARD, J. H. 1966 *J. Fluid Mech.* **25**, 401

GERRARD, J. H. 1972 *IUTAM–IAHR Symp. on Flow-Induced Structure Vibration, Karlsruhe*, paper B 4.

GOLDSTEIN, R. J., ERIKSEN, V. L., OLSON, R. M. & ECKERT, E. R. G. 1970 *J. Basic Engng, Trans. A.S.M.E.* D **92**, 732.

HONJI, H. & TANEDA, S. 1969 *J. Phys. Soc. Japan*, **27**, 1668.

ROSHKO, A. & LAU, J. C. 1965 *Proc. Heat Transfer Fluid Mech. Inst.* (ed. A. F. Charwat), p. 157. Stanford University Press.

TANEDA, S. & HONJI, H. 1971 *J. Phys. Soc. Japan*, **30**, 262.

TANI, I., IUCHI, M. & KOMODA, H. 1961 *Aero. Res. Inst., University of Tokyo, Rep.* no. 364, 1.

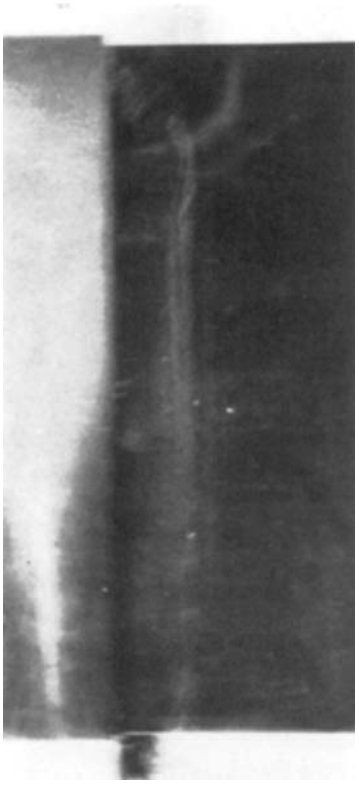

FIGURE 2. Side view of the flow showing the two-dimensionality at $R = 248$ ($U = 1{\cdot}43$ cm/s). Only the upper half of the test section is shown.

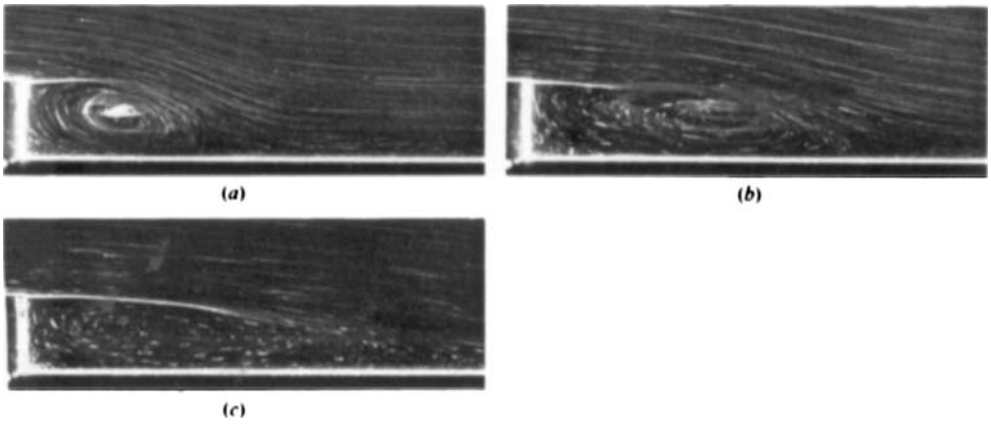

FIGURE 3. Timewise development of streamlines at $R = 99{\cdot}6$ ($U = 0{\cdot}680$ cm/s). (*a*) $Ut/h = 5{\cdot}12$, (*b*) $Ut/h = 12{\cdot}4$, (*c*) $Ut/h = 41{\cdot}7$.

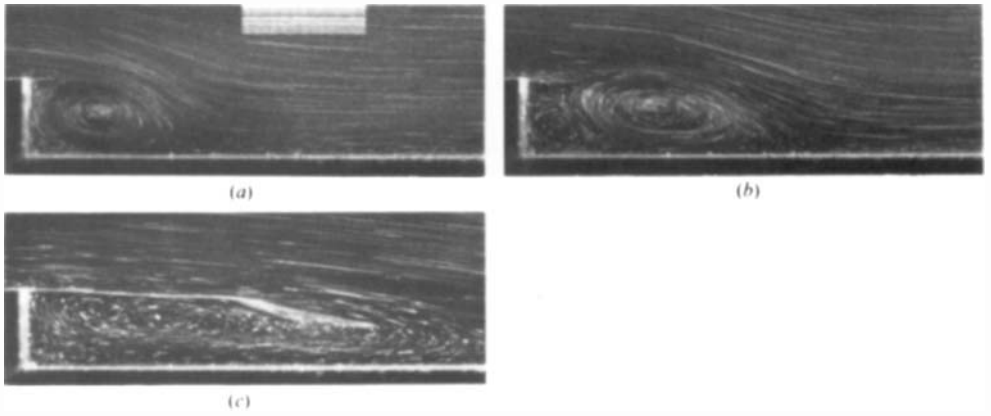

FIGURE 4. As figure 3, but at a slightly larger Reynolds number of 153 (U = 0·956 cm/s). (*a*) Ut/h = 3·34, (*b*) Ut/h = 8·48, (*c*) Ut/h = 31·6.

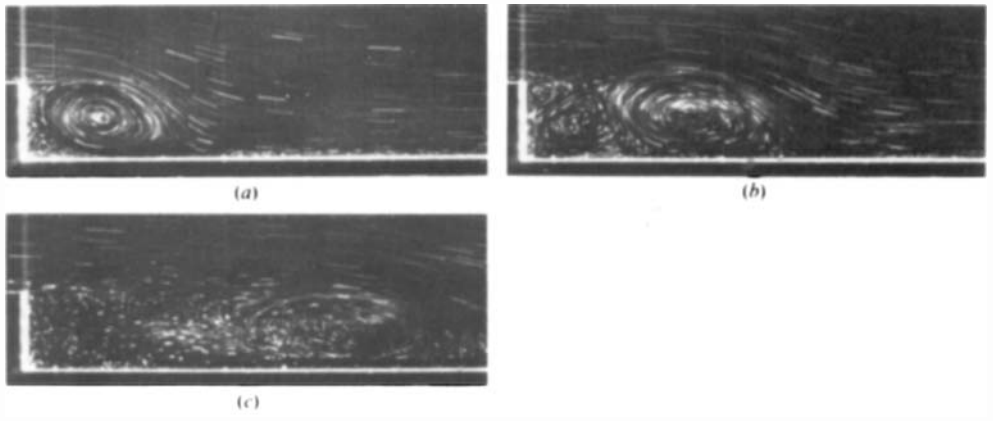

FIGURE 5. Streamline evolution at a relatively large Reynolds number of 304 (U = 1·93 cm/s). (*a*) Ut/h = 3·86, (*b*) Ut/h = 10·5, (*c*) Ut/h = 23·8.

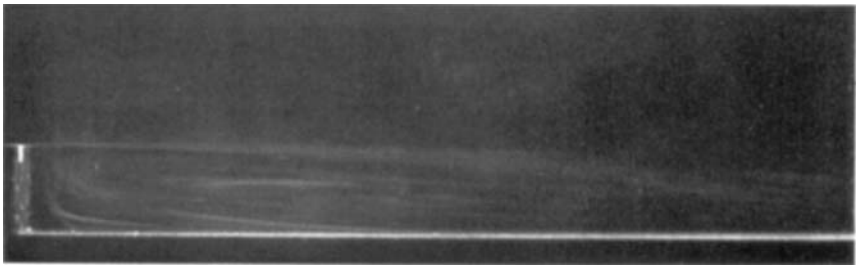

FIGURE 6. A steady recirculation region at $R = 301$ ($U = 1{\cdot}96$ cm/s, $Ut/h = 84{\cdot}2$).

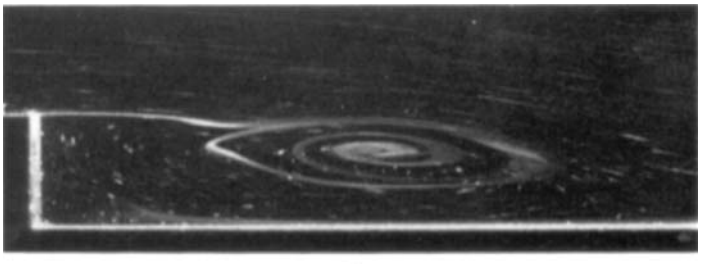

(*a*)

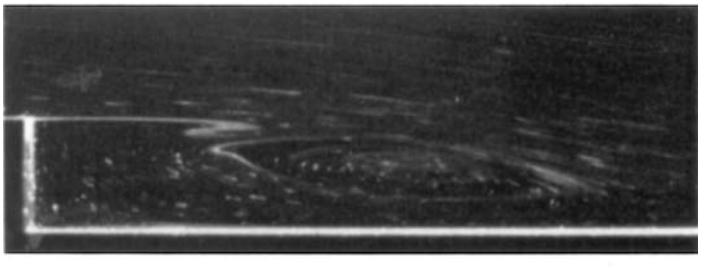

(*b*)

FIGURE 10. Formation of a kink in a filament. (*a*) $R = 135$, $Ut/h = 17{\cdot}0$, (*b*) $R = 146$, $Ut/h = 18{\cdot}4$.

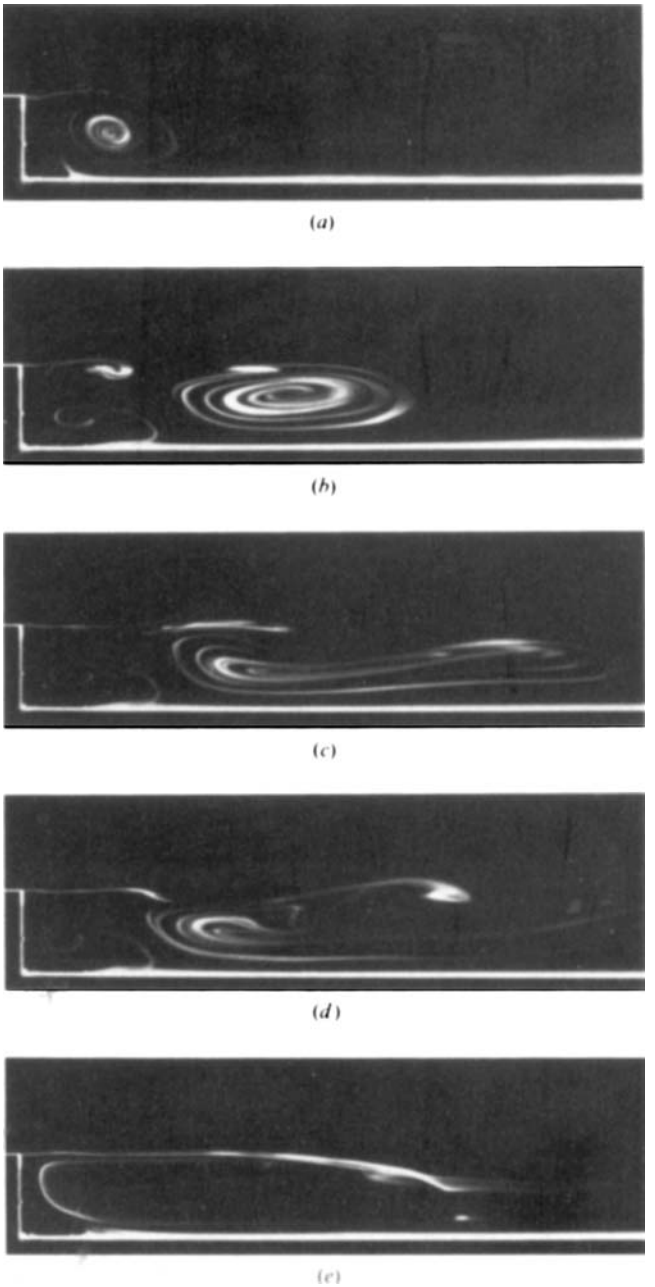

FIGURE 12. Development of filaments at $R = 283$ ($U = 1{\cdot}68$ cm/s). (*a*) $Ut/h = 4{\cdot}77$, (*b*) $Ut/h = 13{\cdot}9$, (*c*) $Ut/h = 18{\cdot}4$, (*d*) $Ut/h = 23{\cdot}0$, (*e*) $Ut/h = 45{\cdot}7$.

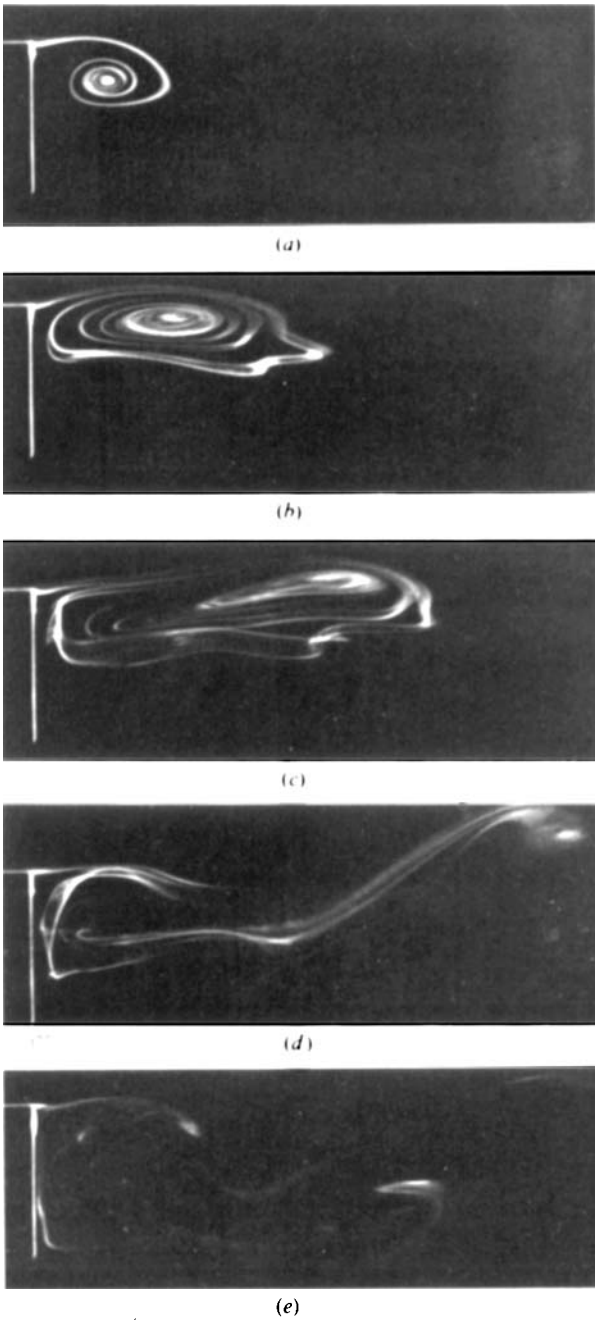

FIGURE 14. Development of filaments behind the model without a downstream wall at $R = 284$ ($U = 1{\cdot}68$ cm/s). (*a*) $Ut/h = 4{\cdot}82$, (*b*) $Ut/h = 14{\cdot}0$, (*c*) $Ut/h = 18{\cdot}6$, (*d*) $Ut/h = 23{\cdot}2$, (*e*) $Ut/h = 46{\cdot}2$.